IEEE Access
Multidisciplinary | Rapid Review | Open Access Journal

Received December 23, 2020, accepted January 4, 2021, date of publication January 8, 2021, date of current version January 25, 2021.

Digital Object Identifier 10.1109/ACCESS.2021.3050258

A Time Optimal Trajectory Planning Method for Double-Pendulum Crane Systems With Obstacle Avoidance

WA ZHANG, HE CHEN, (Member, IEEE), HAIYONG CHEN, AND WEIPENG LIU
School of Artificial Intelligence, Hebei University of Technology, Tianjin 300401, China

Corresponding author: He Chen (chenh@hebut.edu.cn)

This work was supported in part by the National Natural Science Foundation of China under Grant 61903120, Grant U20A20198, Grant 61941303, and Grant 62073118; in part by the Natural Science Foundation of Hebei Province under Grant F2020202006 and Grant F2020202009; and in part by the Key Research and Development Project of Hebei Province under Grant 20271804D.

ABSTRACT For a crane system, when the payload is too large to be seen as a mass point, or the hook mass cannot be directly ignored, it performs more like a double-pendulum crane system, instead of a single-pendulum crane system. Due to many factors, the working environment of the industrial crane system is complex. Obstacles sometimes appear in the movement path of the payload, which affects the normal operation of the crane system and may cause accidents like collisions. To handle this issue, we propose a time optimal trajectory planning method for the double-pendulum crane system with obstacle avoidance, which ensures the objective of obstacle avoidance by the payload hoisting/lowering. During the trajectory planning process, a series of physical constraints, including the trolley velocity constraints, the trolley acceleration constraints, the payload's swing angle constraints and the hook's swing angle constraints are considered. It can improve the safety of the crane system during the entire working process and the transportation efficiency is also improved at the same time. Finally, the effectiveness of the proposed method is verified by simulations.

INDEX TERMS Double-pendulum cranes, obstacle avoidance, trajectory planning, underactuated systems.

I. INTRODUCTION

With the improvement of industrialization, the level of industrial mechanization and automation is also improved. Cranes are an important means of transportation. They can be applied in many fields, such as cargo hoisting on ships [1], container hoisting on docks [2]–[4], parts hoisting in factories and so forth [5]–[7]. At present, most cranes are manually operated. However, due to the underactauted characteristics of crane systems, even experienced workers cannot eliminate payload's swing quickly. Therefore, it is necessary to design automatic control methods. In recent decades, the research on the automatic control method of crane system has practical significance and wide application value, which has attracted researchers' attention.

Generally speaking, the crane system has two control objectives: the first is to make the payload reach the target position quickly and accurately; the second is to suppress the payload's swing. At present, most researchers ignore the hook mass and regard the crane as a single-pendulum system. They build simplified single-pendulum models based on the coupling between the trolley and the payload. Most existing methods are based on single-pendulum models, such as trajectory planning [8]–[10], energy-based control [11], [12], adaptive control [13]–[15], sliding-mode control [16], intelligent control [17]–[20], and innovation control [21]. Some researches have achieved good control performance. In some practical situations, the single-pendulum model is no longer effective, such as: 1) the hook mass is comparable with the payload mass; 2) the size of the payload carried by cranes are large (e.g., containers, steel pipes, fan blades); and 3) the rope connecting the hook and the payload are long. At this time, the crane system presents double-pendulum characteristics. In other words, we need to consider the payload's swing around the hook. Due to the existance of the double-pendulum performance, the above-mentioned single-pendulum crane control methods are not suitable, and only few literatures have reported control methods designed

The associate editor coordinating the review of this manuscript and approving it for publication was Choon Ki Ahn.

for double-pendulum cranes. For the double-pendulum crane, since one more unactuated state variable appears while the control inputs remain the same, the control problem is much more difficult than that of the single-pendulum crane. In [22], under the premise of considering various constraints, the transportation time function as the performance index is given and solved by the bisection-based method to obtain the desired trajectory. By using the adaptive proportional-derivative sliding mode control (APD-SMC) law, the coupling behavior between the trolley and the payload is enhanced and the transient performance is improved in [23]. Reference [24] shows an adaptive design which can make a fixed sliding mode surface active to search the state trajectory and improve the cart tracking precision. Qian *et al*. put forward an single-input-rule module (SIRMs) for fuzzy inference models [25]. The SIRMs can decrease the number of fuzzy rules. Tuan uses neural networks to estimate uncertain parameters and unknown winds [26]. By applying these methods, the performance and effectiveness of the double-pendulum crane control system are investigated.

In the industrial production, cranes not only need to complete the transportation objective, but also need to face the complex and demanding production environment. Sometimes obstacles appear on the movement path of the payload. If they cannot be avoided in time, accidents will occur. Therefore, we need to consider not only the payload swing problem, but also the payload obstacle avoidance problem. During the past decades, few methods have been applied to crane systems with obstacle avoidance.

On the one hand, some scholars studied on assistance obstacle avoidance control methods. Yang *et al.* studied on a safety alarm device for overhead crane to prevent impacting persons or objects and used image processing technology to create a video surveillance system [27]. In [28], Hara *et al*. studied on the operational assistance system for avoiding the obstacles collision and suppressing the payload sway. The payload sway can be suppressed by the filtering approach. The effectiveness of the proposed system is verified by the experiments with the laboratory-type overhead traveling crane.

On the other hand, some scholars have proposed some novel obstacle avoidance control methods based on crane dynamics. Gutierrez and Collado analyzed the crane dynamics and proposed a novel control method which uses a virtual one-wired crane that is equivalent to the new two-wired one [29]. Miyoshi *et al.* present the method that deals with path planning for autonomous overhead cranes considering payload rotation [30]. Inomata and Noda studied on an advanced transfer trajectory planning method of 2-dimensional transfer machines with vibrational element such as an overhead traveling crane [31]. Iftikhar *et al*. studied on an optimization-based controller for guiding the crane through arbitrary obstacles [32]. Solving path planning problems with obstacles typically requires a two-stage approach.

In the above references, obstacle avoidance control methods are proposed only for single pendulum crane systems. On the other hand, there is no existing obstacle avoidance control method for double-pendulum crane systems. For the double-pendulum crane, the payload swing is more complex, and it is more difficult to avoid the obstacle when the obstacle appears on the payload moving path. Therefore, it is more important to propose the obstacle avoidance method for double-pendulum crane systems. In order to solve this troublesome problem, in this paper, we propose an effective trajectory planning method for double pendulum crane systems with the consideration of obstacle avoidance. Specifically, through the analysis of the double-pendulum crane model, the crane is shown to be differentially flat and the flatness property are used to deal with couplings between system states. Then a time optimization problem is constructed by considering the requirement of obstacle avoidance and a series of physical constraints, including the trolley velocity constraints, the trolley acceleration constraints, the payload's swing angle constraints, and the hook's swing angle constraints. The constructed optimization problem is solved by a bisection-based method and the optimal transport time is obtained, together with the time optimal trajectory. Simulation results show that this method can achieve the obstacle avoidance objective and the transportation task under physical constraints.

The main contributions of the proposed method are illustrated as follows: This method is an effective trajectory planning method with obstacle avoidance, which is designed for double-pendulum cranes and can improve the system safety. Through analysis of the dynamics and the system kinematic characteristics, it is concluded that the crane system is differentially flat with the payload coordinates as the flat outputs, which is further used to deal with the coupling behavior between state variables more conveniently. During the trajectory planning process, a series of physical constraints are considered to ensure the trackability of the trajectory and further improve the double-pendulum crane system safety. At the same time of avoiding obstacles, the time optimal trajectory is obtained, which can greatly improve the efficiency of the crane system.

II. PROBLEM STATEMENT

The considered double-pendulum crane system is shown in FIGURE 1, whose dynamics are described as follows:

$$\begin{aligned}&(m+m_1+m_2)\ddot{x}+(m_1+m_2)(\ddot{l}_1\sin\theta_1+2\dot{l}_1\cos\theta_1\dot{\theta}_1\\&\quad+l_1\cos\theta_1\ddot{\theta}_1-l_1\sin\theta_1\dot{\theta}_1^2)+m_2l_2(\cos\theta_2\ddot{\theta}_2-\sin\theta_2\dot{\theta}_2^2)\\&=f_x\end{aligned}\tag{1}$$

$$\begin{aligned}&(m_1+m_2)(\ddot{x}\sin\theta_1+\ddot{l}_1-l_1\dot{\theta}_1^2)+m_2l_2[\ddot{\theta}_2\sin(\theta_1-\theta_2)\\&\quad-\dot{\theta}_2^2\cos(\theta_1-\theta_2)]-(m_1g+m_2g)\cos\theta_1=f_l\end{aligned}\tag{2}$$

$$\begin{aligned}&(m_1+m_2)(\ddot{x}l_1\cos\theta_1+2l_1\dot{l}_1\dot{\theta}_1+l_1^2\ddot{\theta}_1)\\&\quad+m_2l_2[l_1\ddot{\theta}_2\cos(\theta_1-\theta_2)+l_1\dot{\theta}_2^2\sin(\theta_1-\theta_2)]\\&\quad+l_1\sin\theta_1(m_1g+m_2g)=0\end{aligned}\tag{3}$$

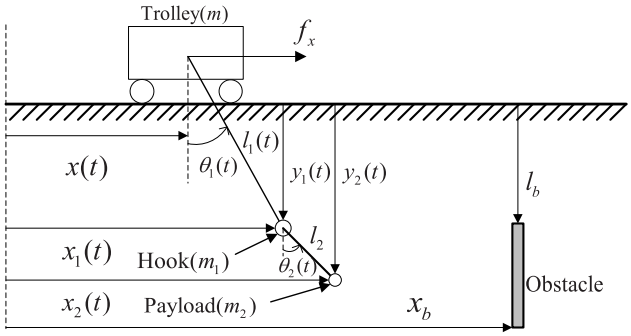

FIGURE 1. Illustration for a double-pendulum crane system with obstacle.

$$m_2 l_2[\ddot{x}\cos\theta_2 + (\ddot{l}_1 - l_1\dot{\theta}_1^2)\sin(\theta_1-\theta_2) + l_2\ddot{\theta}_2 + \cos(\theta_1-\theta_2)(2\dot{l}_1\dot{\theta}_1 + l_1\ddot{\theta}_1)] + m_2 l_2 g\sin\theta_2 = 0 \quad (4)$$

where m, m_1, m_2 represent masses of the trolley, the hook and the payload, respectively, $x(t)$ denotes the trolley position, $l_1(t)$ and l_2 denote the rope length and the distance between the hook center and the payload center, respectively, $\theta_1(t)$ and $\theta_2(t)$ denote the hook's swing angle and the payload's swing angle, respectively, $f_x(t)$ and $f_l(t)$ represent the trolley actuating force and the payload hoisting/lowering actuating force, respectively, and g is the gravity acceleration constant.

Due to the fact that the working environment is very complicated, obstacles sometimes appear in moving path of the payload as shown in FIGURE 1. If the obstacle avoidance objective is not considered, accidents like collisions may occur, which is dangerous. For this reason, we seek to design an effective trajectory planning method for double-pendulum crane systems with the consideration of obstacle avoidance to ensure safety and avoid possible collisions. Considering the requirements of accurate transportation, swing suppression, and obstacle avoidance, the control objectives are described as follows:

- Control the trolley from the initial position x_i to the target position x_d.
- As shown in FIGURE 1, assume that the obstacle appears at x_b, the payload should be hoisted in order to achieve the obstacle avoidance objective. When the payload horizontal position $x_2(t)$ reaches x_b, the payload vertical position $y_2(t)$ reaches the obstacle top position l_b from its initial vertical position l_i. To complete the transportation task, when the payload passes the obstacle, it needs to be lowered. When the payload reaches its desired position x_d, the payload vertical position $y_2(t)$ should reach its initial value l_i.
- Eliminate the hook's swing $\theta_1(t)$ and the payload's swing $\theta_2(t)$.

In order to achieve the above control objectives, we will propose an effective method in the next section.

III. TRAJECTORY PLANNING

A. FLAT OUTPUT CONSTRUCTION

By using the small angle assumption[1], (3) and (4) are linearized as follows:

$$(m_1+m_2)(\ddot{x}l_1 + 2\dot{l}_1\dot{\theta}_1 + l_1{}^2\ddot{\theta}_1 + l_1\theta_1 g) + m_2 l_1 l_2\ddot{\theta}_2 = 0 \quad (5)$$

$$\ddot{x} + \ddot{l}_1\theta_1 - \ddot{l}_1\theta_2 + l_2\ddot{\theta}_2 + 2\dot{l}_1\dot{\theta}_1 + l_1\ddot{\theta}_1 + g\theta_2 = 0 \quad (6)$$

At the same time, one can express the coordinates of the hook as follows:

$$x_1 = x + l_1\sin\theta_1,\ y_1 = l_1\cos\theta_1 \quad (7)$$

where $x_1(t)$ and $y_1(t)$ are the hook horizontal position and the hook vertical position, respectively.

Similarly, one can express the coordinates of the payload as follows:

$$x_2 = x + l_1\sin\theta_1 + l_2\sin\theta_2 \quad (8)$$

$$y_2 = l_1\cos\theta_1 + l_2\cos\theta_2 \quad (9)$$

where $x_2(t)$ and $y_2(t)$ represent the payload horizontal position and the payload vertical position, respectively. (7)–(9) can also be linearized as follows:

$$x_1 = x + l_1\theta_1,\ y_1 = l_1 \quad (10)$$

$$x_2 = x + l_1\theta_1 + l_2\theta_2 \quad (11)$$

$$y_2 = l_1 + l_2 \quad (12)$$

Taking the time derivative of (11) and (12), it is found that

$$\dot{x}_2 = \dot{x} + \dot{l}_1\theta_1 + l_1\dot{\theta}_1 + l_2\dot{\theta}_2 \quad (13)$$

$$\dot{y}_2 = \dot{l}_1 \quad (14)$$

Taking the time derivative of (13) and (14) again, it is further obtained that

$$\ddot{x}_2 = \ddot{x} + \ddot{l}_1\theta_1 + 2\dot{l}_1\dot{\theta}_1 + l_1\ddot{\theta}_1 + l_2\ddot{\theta}_2 \quad (15)$$

$$\ddot{y}_2 = \ddot{l}_1 \quad (16)$$

Substituting (16) into (15), one can obtain

$$\ddot{x}_2 = \ddot{x} + \ddot{y}_2\theta_1 + 2\dot{l}_1\dot{\theta}_1 + l_1\ddot{\theta}_1 + l_2\ddot{\theta}_2 \quad (17)$$

Substituting (17) into (5), one has

$$(m_1+m_2)l_1(\ddot{x}_2 - \ddot{y}_2\theta_1 + \theta_1 g) - m_1 l_1 l_2\ddot{\theta}_2 = 0 \quad (18)$$

Since the rope length $l_1(t)$ would not be equal to zero in practice, (18) can be further simplified into the following structure

$$(m_1+m_2)(\ddot{x}_2 - \ddot{y}_2\theta_1 + \theta_1 g) - m_1 l_2\ddot{\theta}_2 = 0 \quad (19)$$

Substituting (15) and (16) into (6), one has

$$\ddot{x}_2 - \ddot{y}_2\theta_2 + g\theta_2 = 0 \quad (20)$$

[1]When the swing angle is small enough, the kinematic equation can be linearized with the approximations of $\sin\theta_1 \simeq \theta_1$, $\sin\theta_2 \simeq \theta_2$, $\cos\theta_1 \simeq 1$, $\cos\theta_2 \simeq 1$, $\sin(\theta_1-\theta_2)\dot{\theta}_1^2 \simeq 0$ and $\sin(\theta_1-\theta_2)\dot{\theta}_2^2 \simeq 0$ [33], [34].

From (19) and (20), it is found that

$$\theta_1 = \frac{\ddot{x}_2}{\ddot{y}_2 - g} - \frac{m_1 l_2 \ddot{\theta}_2}{(m_1 + m_2)(\ddot{y}_2 - g)} \tag{21}$$

$$\theta_2 = \frac{\ddot{x}_2}{\ddot{y}_2 - g} \tag{22}$$

Substituting (22) into (21), one has

$$\theta_1 = \frac{\ddot{x}_2}{\ddot{y}_2 - g} - \frac{m_1 l_2 (x_2^{(4)} \ddot{y}_2 - x_2^{(4)} g - \ddot{x}_2 y_2^{(3)})}{(m_1 + m_2)(\ddot{y}_2 - g)^3} - \frac{2 m_1 l_2 y_2^{(3)} x_2^{(3)} g}{(m_1 + m_2)(\ddot{y}_2 - g)^4} \tag{23}$$

Substituting (22) and (23) into (11), one can derive the following result:

$$x = x_2 - l_2 \frac{\ddot{x}_2}{\ddot{y}_2 - g} + (l_2 - y_2)\left[\frac{\ddot{x}_2}{\ddot{y}_2 - g} - \frac{m_1 l_2 (x_2^{(4)} \ddot{y}_2 - x_2^{(4)} g - \ddot{x}_2 y_2^{(3)})}{(m_1 + m_2)(\ddot{y}_2 - g)^3} - \frac{2 m_1 l_2 y_2^{(3)} x_2^{(3)} g}{(m_1 + m_2)(g - \ddot{y}_2)^4}\right] \tag{24}$$

It can be concluded that based on (12) and (22)–(24), all system state variables, i.e., $l_1(t)$, $x(t)$, $\theta_1(t)$, $\theta_2(t)$ can be expressed by $x_2(t)$ and $y_2(t)$. Therefore, we can draw the conclusion that the crane system is differentially flat with the payload coordinates as the flat outputs.

B. OPTIMIZATION PROBLEM CONSTRUCTION

In order to obtain the optimal transportation time, we first consider the conditions as follows:

1) At the initial moment $t = 0$, the trolley is at the initial position x_i, and its speed, acceleration and jerk shall all be zero. The hook's swing angle and angular velocity are both zero. The payload's swing angle and angular velocity are also both zero. At the final moment $t = T$, the trolley arrives at the target position x_d, and its speed, acceleration and jerk shall all be zero. At the same time, the payload reaches the target position. The payload and the hook stop swinging. The payload's swing angle and angular velocity are both zero. The hook's swing angle and angular velocity are also both zero. Then we have

$$\begin{aligned} &x(0) = x_i, \quad \dot{x}(0) = 0, \\ &\ddot{x}(0) = 0, \quad x^{(3)}(0) = 0 \end{aligned} \tag{25}$$

$$\begin{aligned} &x(T) = x_d, \quad \dot{x}(T) = 0, \\ &\ddot{x}(T) = 0, \quad x^{(3)}(T) = 0 \end{aligned} \tag{26}$$

$$\begin{aligned} &\theta_1(0) = 0, \quad \dot{\theta}_1(0) = 0, \\ &\theta_1(T) = 0, \quad \dot{\theta}_1(T) = 0 \end{aligned} \tag{27}$$

$$\begin{aligned} &\theta_2(0) = 0, \quad \dot{\theta}_2(0) = 0, \\ &\theta_2(T) = 0, \quad \dot{\theta}_2(T) = 0 \end{aligned} \tag{28}$$

2) To achieve obstacle avoidance, the payload should be hoisted at the first. At the initial moment $t = 0$, the payload initial vertical position is l_i. The payload initial vertical velocity, acceleration and jerk should also be zero. When the payload horizontal position $x_2(t)$ reaches x_b at time $t = t_s$, the payload vertical position should reach l_b at the top of the obstacle. The payload vertical velocity, acceleration and jerk ought to be zero. When the payload passes the obstacle, it starts to be lowered. When the payload reaches the target position at time $t = T$, the payload vertical position is l_i. In addition, the payload vertical velocity, acceleration, and jerk should also be zero at time $t = T$. Then we have

$$\begin{aligned} &y_2(0) = l_i, \ \dot{y}_2(0) = 0, \ \ddot{y}_2(0) = 0, \ y_2^{(3)}(0) = 0, \\ &y_2(t_s) = l_b, \ \dot{y}_2(t_s) = 0, \ \ddot{y}_2(t_s) = 0, \ y_2^{(3)}(t_s) = 0, \\ &y_2(T) = l_i, \ \dot{y}_2(T) = 0, \ \ddot{y}_2(T) = 0, \ y_2^{(3)}(T) = 0 \end{aligned} \tag{29}$$

3) To ensure the trackability of the planned trajectory, the amplitude of the trolley speed and acceleration needs to be kept within suitable ranges. At the same time, in order to ensure the safety in the entire transportation process, the payload's swing angle, hook's swing angle and their corresponding angular velocities in the entire process need to be kept in corresponding suitable ranges to avoid danger caused by large swings, which indicates that

$$|\dot{x}(t)| \le v_{\max}, \quad |\ddot{x}(t)| \le a_{\max} \tag{30}$$

$$|\theta_1| \le \theta_{1\max}, \quad |\dot{\theta}_1| \le \omega_{1\max} \tag{31}$$

$$|\theta_2| \le \theta_{2\max}, \quad |\dot{\theta}_2| \le \omega_{2\max} \tag{32}$$

where $v_{\max}$, $a_{\max}$, $\theta_{1\max}$, $\omega_{1\max}$, $\theta_{2\max}$, $\omega_{2\max}$ represent the permitted trolley velocity, acceleration, hook's swing angle, hook angular velocity, payload's swing angle, and payload angular velocity amplitudes, respectively.

After that, substituting (24) into (25) and (26), and doing some calculations, we have the following results:

$$\begin{aligned} &x_2(0) = x_i, \ \dot{x}_2(0) = \ddot{x}_2(0) = x_2^{(3)}(0) = 0, \\ &x_2^{(4)}(0) = x_2^{(5)}(0) = x_2^{(6)}(0) = x_2^{(7)}(0) = 0, \\ &x_2(T) = x_i, \ \dot{x}_2(T) = \ddot{x}_2(T) = x_2^{(3)}(T) = 0, \\ &x_2^{(4)}(T) = x_2^{(5)}(T) = x_2^{(6)}(T) = x_2^{(7)}(T) = 0 \end{aligned} \tag{33}$$

Substituting (22) into (32), one has

$$\left|\frac{\ddot{x}_2}{\ddot{y}_2 - g}\right| \le \theta_{2\max} \tag{34}$$

$$\left|\frac{x_2^{(3)}}{\ddot{y}_2 - g} - \frac{\ddot{x}_2 y_2^{(3)}}{(\ddot{y}_2 - g)^2}\right| \le \omega_{2\max} \tag{35}$$

Substituting (23) into (31), one can obtain

$$\left|\frac{\ddot{x}_2}{\ddot{y}_2 - g} - \frac{m_1 l_2 (x_2^{(4)} \ddot{y}_2 - x_2^{(4)} g - \ddot{x}_2 y_2^{(3)})}{(m_1 + m_2)(\ddot{y}_2 - g)^3} - \frac{2 m_1 l_2 y_2^{(3)} x_2^{(3)} g}{(m_1 + m_2)(\ddot{y}_2 - g)^4}\right| \le \theta_{1\max} \tag{36}$$

$$\left|\frac{x_2^{(3)}}{\ddot{y}_2-g}-\frac{\ddot{x}_2y_2^{(3)}}{(\ddot{y}_2-g)^2}\right.$$
$$-\frac{m_1l_2}{m_1+m_2}\left[\frac{x_2^{(5)}(\ddot{y}_2-g)+y_2^{(3)}(x_2^{(4)}-x_2^{(3)})-x_2^{(5)}g}{(\ddot{y}_2-g)^3}\right.$$
$$\left.-\frac{3y_2^{(3)}(x_2^{(4)}\ddot{y}_2-x_2^{(4)}g-\ddot{x}_2y_2^{(3)})}{(\ddot{y}_2-g)^4}\right]$$
$$-\frac{2m_1l_2}{m_1+m_2}\left[\frac{y_2^{(4)}x_2^{(3)}g+y_2^{(3)}x_2^{(4)}g}{(\ddot{y}_2-g)^4}\right.$$
$$\left.\left.-\frac{4y_2^{(3)}y_2^{(3)}x_2^{(3)}g}{(\ddot{y}_2-g)^5}\right]\right|\le\omega_{1\max}\tag{37}$$

Using the equation (24), we can write (30) by

$$\left|\dot{x}_2-\frac{x_2^{(3)}y_2+\ddot{x}_2\dot{y}_2}{\ddot{y}_2-g}+\frac{\ddot{x}_2y_2y_2^{(3)}}{(\ddot{y}_2-g)^2}\right.$$
$$+\frac{m_1l_2}{m_1+m_2}\left[\frac{(x_2^{(5)}\ddot{y}_2+x_2^{(4)}y_2^{(3)}-x_2^{(5)}g)(y_2-l_2)}{(\ddot{y}_2-g)^3}\right.$$
$$-\frac{(x_2^{(3)}y_2^{(3)}+\ddot{x}_2y_2^{(4)})(y_2-l_2)-(x_2^{(4)}\ddot{y}_2-x_2^{(4)}g-\ddot{x}_2y_2^{(3)})\dot{y}_2}{(\ddot{y}_2-g)^3}$$
$$+\frac{3y_2^{(3)}(x_2^{(4)}\ddot{y}_2-x_2^{(4)}g-\ddot{x}_2y_2^{(3)})(y_2-l_2)}{(\ddot{y}_2-g)^4}$$
$$\left.+2g\frac{(y_2^{(4)}x_2^{(3)}+y_2^{(3)}x_2^{(4)})(y_2-l_2)+y_2^{(3)}x_2^{(3)}\dot{y}_2}{(\ddot{y}_2-g)^4}\right]$$
$$\left.-\frac{8m_1l_2gx_2^{(3)}y_2^{(3)^2}(y_2-l_2)}{(m_1+m_2)(\ddot{y}_2-g)^5}\right|\le v_{\max}\tag{38}$$
$$\left|\ddot{x}_2-\frac{x_2^{(4)}y_2+2x_2^{(3)}\dot{y}_2+\ddot{x}_2\ddot{y}_2}{\ddot{y}_2-g}-\frac{2y_2^{(3)}y_2^{(3)}\ddot{x}_2y_2}{(\ddot{y}_2-g)^3}\right.$$
$$+\frac{2x_2^{(3)}y_2y_2^{(3)}+2\ddot{x}_2\dot{y}_2y_2^{(3)}+\ddot{x}_2y_2y_2^{(4)}}{(\ddot{y}_2-g)^2}$$
$$-\frac{m_1l_2}{m_1+m_2}\left[\frac{(x_2^{(6)}\ddot{y}_2+2x_2^{(5)}y_2^{(3)}+x_2^{(4)}y_2^{(4)})(y_2-l_2)}{(\ddot{y}_2-g)^3}\right.$$
$$-\frac{(x_2^{(6)}g+x_2^{(4)}y_2^{(3)}+2x_2^{(3)}y_2^{(4)}+\ddot{x}_2y_2^{(4)})(y_2-l_2)}{(\ddot{y}_2-g)^3}$$
$$+\frac{2\dot{y}_2(x_2^{(5)}\ddot{y}_2+x_2^{(4)}y_2^{(3)}-x_2^{(5)}g-x_2^{(3)}y_2^{(3)}-\ddot{x}_2y_2^{(4)})}{(\ddot{y}_2-g)^3}$$
$$+\frac{3y_2^{(3)}(y_2-l_2)(x_2^{(5)}\ddot{y}_2+x_2^{(4)}y_2^{(3)})}{(\ddot{y}_2-g)^4}$$
$$-\frac{3y_2^{(3)}(y_2-l_2)(x_2^{(5)}g+x_2^{(3)}y_2^{(3)}+\ddot{x}_2y_2^{(4)})}{(\ddot{y}_2-g)^4}$$
$$+\frac{\ddot{y}_2(x_2^{(4)}\ddot{y}_2-x_2^{(4)}g-\ddot{x}_2y_2^{(3)})}{(\ddot{y}_2-g)^3}$$
$$-\frac{3\dot{y}_2y_2^{(3)}(x_2^{(4)}\ddot{y}_2-x_2^{(4)}g-\ddot{x}_2y_2^{(3)})}{(\ddot{y}_2-g)^4}$$
$$+\frac{(x_2^{(4)}\ddot{y}_2-x_2^{(4)}g-\ddot{x}_2y_2^{(3)})(3\dot{y}_2y_2^{(3)}+3y_2y_2^{(4)}-3l_2y_2^{(4)})}{(\ddot{y}_2-g)^4}$$
$$-\frac{9y_2^{(3)}y_2^{(3)}(y_2-l_2)(x_2^{(4)}\ddot{y}_2-x_2^{(4)}g-\ddot{x}_2y_2^{(3)})}{(\ddot{y}_2-g)^5}$$
$$+\frac{2g(y_2-l_2)(y_2^{(5)}x_2^{(3)}+2y_2^{(4)}x_2^{(4)}+y_2^{(3)}x_2^{(5)})}{(\ddot{y}_2-g)^4}$$
$$+\frac{2g(2y_2^{(4)}x_2^{(3)}\dot{y}_2+2y_2^{(3)}x_2^{(4)}\dot{y}_2+y_2^{(3)}x_2^{(3)}\ddot{y}_2)}{(\ddot{y}_2-g)^4}$$
$$-\frac{8gy_2^{(3)}(y_2^{(4)}x_2^{(3)}+y_2^{(3)}x_2^{(4)})(y_2-l_2)}{\ddot{y}_2-g^5}$$
$$\left.-\frac{8gy_2^{(3)}y_2^{(3)}x_2^{(3)}\dot{y}_2}{(\ddot{y}_2-g)^5}\right]$$
$$-\frac{2m_1l_2g}{m_1+m_2}\left[\frac{4y_2^{(3)}(y_2^{(4)}x_2^{(3)}+y_2^{(3)}x_2^{(4)})(y_2-l_2)}{(\ddot{y}_2-g)^5}\right.$$
$$+\frac{4y_2^{(3)}x_2^{(3)}\dot{y}y_2^{(3)}+4y_2^{(3)}y_2^{(4)}x_2^{(3)}(y_2-l_2)}{(\ddot{y}_2-g)^5}$$
$$\left.\left.-\frac{20y_2^{(3)}y_2^{(3)}y_2^{(3)}x_2^{(3)}(y_2-l_2)}{(\ddot{y}_2-g)^6}\right]\right|\le a_{\max}\tag{39}$$

So far, all the constraints shown in (29) and (33)–(39) are converted into constraints on the payload's horizontal and vertical coordinates $x_2(t)$ and $y_2(t)$. We can construct a time optimization problem as

$$\begin{aligned}&\text{minimize}\quad T\\&\text{subject to (29) and (33)}-\text{(39)}.\end{aligned}\tag{40}$$

In the next section, we will solve the time optimization problem and obtain the trolley and rope trajectories.

C. TRAJECTORY PLANNING

By analyzing (33), it is found that there are 16 equality constraints on $x_2(t)$. We choose a 15-order polynomial function to represent $x_2(t)$, which is indicated as follows:

$$x_2(t)=(x_d-x_i)\sum_{i=0}^{15}\alpha_i\left(\frac{t}{T}\right)^i+x_i\tag{41}$$

where α_i's, $i=\{0,1,\ldots,15\}$ are to-be-determined parameters. Then the nth-order derivative of $x_2(t)$ gives the result as follows:

$$x_2^{(n)}(t)=(x_d-x_i)\sum_{i=n}^{15}\alpha_i\frac{i!}{(i-n)!}\left(\frac{1}{T}\right)^n\left(\frac{t}{T}\right)^{i-n}\tag{42}$$

Substituting (41) and (42) into (33) and making some calculations, we can get

$$\begin{aligned}&\alpha_0=\alpha_1=\alpha_2=\alpha_3=\alpha_4=\alpha_5=\alpha_6=\alpha_7=0,\\&\alpha_8=6435,\ \ \alpha_9=-40040,\ \alpha_{10}=108108,\\&\alpha_{11}=-163800,\ \ \alpha_{12}=150150,\ \alpha_{13}=-83160,\\&\alpha_{14}=25740,\ \ \alpha_{15}=-3432\end{aligned}\tag{43}$$

By analyzing (29), it is found that there are 8 equality constraints on $y_2(t)$. We choose a 7-order polynomial function

to represent $y_2(t)$, which is indicated as follows:

$$y_2(t) = \begin{cases} (l_b - l_i)\sum_{i=0}^{7} \beta_i (\frac{t}{t_s})^i + l_i, & t \in [0, t_s) \\ (l_i - l_b)\sum_{i=0}^{7} \beta_i (\frac{t - t_s}{T - t_s})^i + l_b, & t \in [t_s, T] \end{cases} \tag{44}$$

where β_i's, $i = \{0, 1, \ldots, 7\}$ are to-be-determined parameters and t_s is the time when the payload reaches the horizontal position x_b. Substituting (44) into (29) and making some calculations, we can get

$$\begin{aligned} &\beta_0 = \beta_1 = \beta_2 = \beta_3 = 0, \\ &\beta_4 = 35, \ \ \beta_5 = -84, \ \ \beta_6 = 70, \ \ \beta_7 = -20 \end{aligned} \tag{45}$$

In order to solve the time optimization problem and then finish the optimal trajectory planning, we choose to use a bisection-based method, whose application process is shown in **Algorithm 1** by pseudo codes, where T_1 and T_2 represent the lower and upper bounds of the transportation time, respectively, T^* represents the optimal transportation time, and $\delta \in \Re^+$ is the allowable error bound.

Algorithm 1 Detailed Processes of Solving the Time Optimization Problem (40)

Input: x_i, x_d, x_b, l_i, l_2, l_b, $v_{\max}$, $a_{\max}$, $\theta_{1\max}$, $\omega_{1\max}$ $\theta_{2\max}$, $\omega_{2\max}$, T_1, T_2, δ.
Output: T^*.

```
while T_2 − T_1 > δ do
    set: T = (T_1 + T_2)/2
    if (34)–(39) are all satisfied then
        T_2 = T
    else
        T_1 = T
    end if
end while
T* = T_2.
```

Using the **Algorithm 1**, we get the optimal transportation time T^*, while using (24) and (12), the optimal trolley trajectory and the rope trajectory are shown as

$$x_r(t) = \begin{cases} x_2 - l_2 \dfrac{\ddot{x}_2}{\ddot{y}_2 - g} \\ +(l_2 - y_2)\left[\dfrac{\ddot{x}_2}{\ddot{y}_2 - g} - \dfrac{2m_1 l_2 y_2^{(3)} x_2^{(3)} g}{(m_1 + m_2)(g - \ddot{y}_2)^4}\right. \\ \left. - \dfrac{m_1 l_2 (x_2^{(4)} \ddot{y}_2 - x_2^{(4)} g - \ddot{x}_2 y_2^{(3)})}{(m_1 + m_2)(\ddot{y}_2 - g)^3}\right], \ t \in [0, T^*] \\ x_d, \ t > T^* \end{cases} \tag{46}$$

$$l_{1r}(t) = \begin{cases} y_2 - l_2, & t \in [0, T^*] \\ l_i - l_2, & t > T^* \end{cases} \tag{47}$$

At this point, the entire trajectory planning process is completed. On the other hand, from the detailed process of the proposed method, it is concluded that this is no limitation of the payload mass for the proposed trajectory planning method. The obstacle avoidance reference trajectory can be obtained for the payload with any mass. Thus there is no mass limit for the payload in the simulations. In practical application, the payload mass may be limited by considering the crane payload capacity.

IV. SIMULATION RESULTS

In this section, the effectiveness of the proposed method will be verified by numerical simulations. Each physical parameter of the double-pendulum crane is set as follows:

$$\begin{aligned} &m = 20\ \text{kg}, \ \ m_1 = 5\ \text{kg}, \ \ m_2 = 1\ \text{kg}, \\ &l_i = 2.6\ \text{m}, \ \ l_2 = 0.4\ \text{m}, \ \ l_b = 0.8\ \text{m}, \ \ g = 9.8\ \text{m/s}^2, \\ &x_i = 0\ \text{m}, \ \ x_b = 0.6\ \text{m}, \ \ x_d = 1.5\ \text{m} \end{aligned}$$

The permitted amplitudes are selected as

$$\begin{aligned} &v_{\max} = 0.5\ \text{m/s}, \ \ a_{\max} = 0.5\ \text{m}^2/\text{s}, \\ &\theta_{1\max} = \theta_{2\max} = 2\ \text{deg}, \ \ \omega_{1\max} = \omega_{2\max} = 5\ \text{deg/s} \end{aligned}$$

The parameters in **Algorithm 1** are set as follows:

$$T_1 = 0\ \text{s}, \ T_2 = 20\ \text{s}, \ \delta = 0.0001$$

By utilizing MATLAB® [35], the time optimization problem is solved with the optimal transportation time as $T^* = 9.4147$ s, and at the same time, we get $t_s = 4.4045$ s. To verify the effectiveness of trajectory planning, proportional-derivative (PD) controllers are used to track the trajectory, which are shown as

$$\begin{aligned} F_x &= -k_{p1}(x - x_r) - k_{d1}(\dot{x} - \dot{x}_r) \\ F_l &= -k_{p2}(l_1 - l_{1r}) - k_{d2}(\dot{l}_1 - \dot{l}_{1r}) - m_1 g - m_2 g \end{aligned}$$

where $k_{p1}, k_{d1}, k_{p2}, k_{d2} \in \Re^+$ are positive control gains. k_{p1} (or k_{p2}) is the proportional gain of PD control method. If we choose a larger k_{p1} (or k_{p2}), it will take a shorter convergence time to track trajectory. However, if k_{p1} (or k_{p2}) is selected too large, the unexpected overshoots of $x_2(t)$ and $y_2(t)$ will happen. k_{d1} (or k_{d2}) is the differential gain of PD control method. If we choose a larger k_{d1} (or k_{d2}), it will cost a longer convergence time to track trajectory. At the same time, larger k_{d1} (or k_{d2}) will help reduce overshoots and oscillations. After carefully tunning, we find satisfactory performances can be obtained if we follow: $k_{p1} = 200, k_{d1} = 100$, $k_{p2} = 1000$, and $k_{d2} = 100$.

All simulations are implemented using the Simulink® toolbox of MATLAB® [36]. The simulation results are show in FIGURES 2–5. In FIGURE 2, the red dashed line, the red dashed-dotted line, and the red dotted line represent the trolley reference trajectory, the rope length reference trajectory, and swing angle constraints, respectively. In FIGURE 3, the red dashed line and the red dashed-dotted line represent trolley velocity constraints and trolley acceleration constraints, respectively. In FIGURE 4, the red dashed line and the red dashed-dotted line represent hook's angular velocity constrains and payload's angular velocity constrains, respectively.

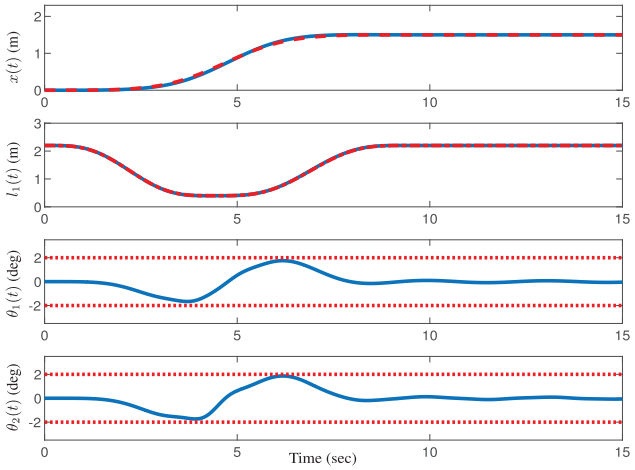

FIGURE 2. Simulation results (the trolley displacement, the rope length, the hook's swing angle, and the payload's swing angle). Black solid line: simulation results; red dashed line: the trolley reference trajectory $x_r(t)$; red dashed- dotted line: the rope length reference trajectory $l_{1r}(t)$; red dotted line: swing angle constraints $\theta_{1\,\max} = \theta_{2\,\max} = 2$ deg.

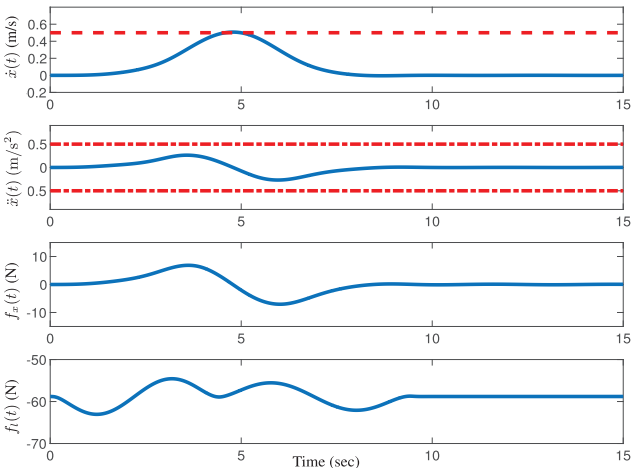

FIGURE 3. Simulation results (the trolley velocity, the trolley acceleration, the trolley actuating force, and the payload hoisting/lowering force). Black solid line: simulation results; red dashed line: trolley velocity constraints $v_{\max} = 0.5$ m/s; red dashed-dotted line: trolley acceleration constraints $a_{\max} = 0.5$ m^2/s.

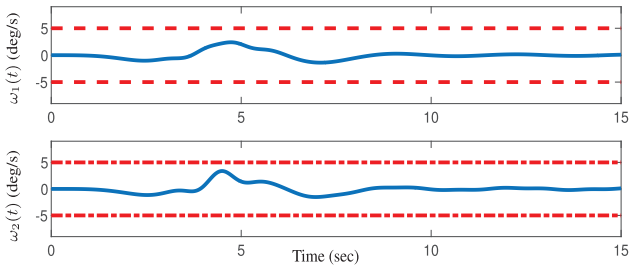

FIGURE 4. Simulation results (the hook's swing angular velocity, and the payload's swing angular velocity). Black solid line: simulation results; red dashed line: hook's angular velocity constraints $\omega_{1\,\max} = 5$ deg/s; red dashed-dotted line: payload's angular velocity constraints $\omega_{2\,\max} = 5$ deg/s.

From FIGURE 2, it is observed that using the method, the trolley reaches its target position rapidly and accurately with nearly no positioning error. The hook's swing angle and payload's swing angle are both suppressed effectively during the transportation. FIGURE 3 shows that the trolley's velocity and acceleration are within the permitted ranges. Additionally, from FIGURE 4, it is also found that the hook's swing angular velocity and the payload's swing angular velocity suppressed effectively. As can be seen from the payload trajectory, the payload can successfully avoid the obstacle in FIGURE 5. Within the optimal transportation time T^*, the trolley and the payload reach the target horizontal position x_d, and at the same time the payload is hoisted to l_b and then lowered to l_i to achieve the obstacle avoidance objective. In other words, the trajectory planning method not only achieves the transportation task, but also ensures the obstacle avoidance. In addition, the payload's swing angle, angular velocity, the hook's swing angle and angular velocity are within suitable ranges.

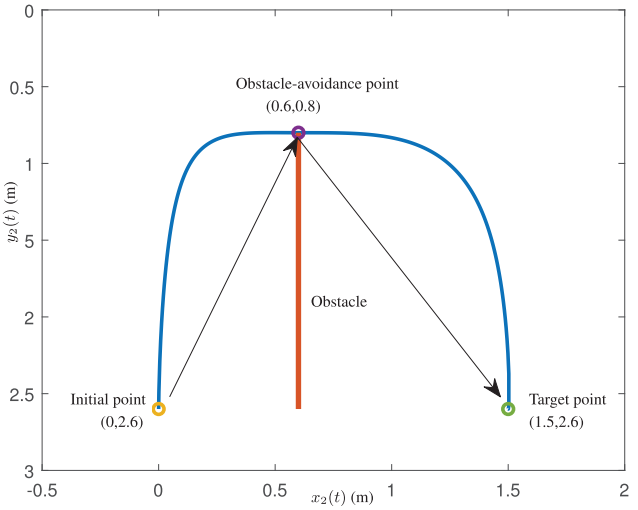

FIGURE 5. Simulation results (payload moving path).

Through numerical simulation tests, it is found that the payload has crossed the obstacle and the crane has completed the transportation task, which also verifies the effectiveness of the proposed method. Due to the lack of necessary experimental equipment, we cannot show the performance of our control method more comprehensively through experiments. At present, we are starting to build the double-pendulum crane testbed. When experimental conditions are available, we will verify the method effectiveness through experiments.

V. CONCLUSION

In order to solve the obstacle avoidance problem of double-pendulum cranes, we propose a trajectory planning method, which can achieve the fast trolley transportation and payload swing suppression, as well as the objective of obstacle avoidance by payload hoisting/lowering. In particular, through the analysis of the crane dynamic model, the double-pendulum crane is shown to be differentially flat with the payload horizontal and vertical positions as the flat outputs. Afterwards, the original trajectory planning is turned into the trajectory planning for flat outputs. By considering the

requirement of obstacle avoidance and a series of physical constraints, a time optimization problem is formulated. Utilizing a bisection-based method, the formulated time optimization problem is solved with the optimal transportation time obtained. Then corresponding optimal trajectories are also obtained. Finally, the effectiveness of the method is verified by simulations. In the following work, we will design an effective tracking strategy to improve the tracking performance and improve the system safety.

ACKNOWLEDGMENT

The authors would like to thank the reviewers and associate editor for the valuable suggestions and comments, which greatly improve the article quality.

REFERENCES

[1] Z. N. Masoud, A. H. Nayfeh, and D. T. Mook, "Cargo pendulation reduction of ship-mounted cranes," *Nonlinear Dyn.*, vol. 35, no. 3, pp. 299–311, Feb. 2004.

[2] N. P. Nguyen, T. N. Phan, and Q. H. Ngo, "Autonomous offshore container crane system using a fuzzy-PD logic controller," in *Proc. 16th Int. Conf. Control, Autom. Syst. (ICCAS)*, Oct. 2016, pp. 1093–1098.

[3] M. Mahrueyan and H. Khaloozadeh, "On the skew and sway control of container cranes," in *Proc. 2nd Int. Conf. Control, Instrum. Autom.*, Dec. 2011, pp. 407–412.

[4] Q. H. Ngo and K.-S. Hong, "Sliding-mode antisway control of an offshore container crane," *IEEE/ASME Trans. Mechatronics*, vol. 17, no. 2, pp. 201–209, Apr. 2012.

[5] J. Smoczek and J. Szpytko, "Particle swarm optimization-based multivariable generalized predictive control for an overhead crane," *IEEE/ASME Trans. Mechatronics*, vol. 22, no. 1, pp. 258–268, Feb. 2017.

[6] M. S. Korytov, V. S. Shcherbakov, and V. V. Titenko, "Analytical solution of the problem of acceleration of cargo by a bridge crane with constant acceleration at elimination of swings of a cargo rope," *J. Phys., Conf. Ser.*, vol. 944, Dec. 2018, Art. no. 012062.

[7] N. Sun, T. Yang, Y. Fang, Y. Wu, and H. Chen, "Transportation control of double-pendulum cranes with a nonlinear quasi-PID scheme: Design and experiments," *IEEE Trans. Syst., Man, Cybern. Syst.*, vol. 49, no. 7, pp. 1408–1418, Jul. 2019.

[8] Z. Wu and X. Xia, "Optimal motion planning for overhead cranes," *IET Control Theory Appl.*, vol. 8, no. 17, pp. 1833–1842, 2014.

[9] H. Chen, P. Yang, and Y. Geng, "A time optimal trajectory planning method for overhead cranes with obstacle avoidance," in *Proc. IEEE/ASME Int. Conf. Adv. Intell. Mechatronics (AIM)*, Jul. 2019, pp. 697–701.

[10] N. Sun, Y. Fang, Y. Zhang, and B. Ma, "A novel kinematic coupling-based trajectory planning method for overhead cranes," *IEEE/ASME Trans. Mechatronics*, vol. 17, no. 1, pp. 166–173, Feb. 2012.

[11] X. Wu and X. He, "Enhanced damping-based anti-swing control method for underactuated overhead cranes," *IET Control Theory Appl.*, vol. 9, no. 12, pp. 1893–1900, Aug. 2015.

[12] N. Sun and Y. Fang, "New energy analytical results for the regulation of underactuated overhead cranes: An end-effector motion-based approach," *IEEE Trans. Ind. Electron.*, vol. 59, no. 12, pp. 4723–4734, Dec. 2012.

[13] C.-Y. Chang, "Adaptive fuzzy controller of the overhead cranes with nonlinear disturbance," *IEEE Trans. Ind. Informat.*, vol. 3, no. 2, pp. 164–172, May 2007.

[14] M.-S. Park, D. Chwa, and M. Eom, "Adaptive sliding-mode antisway control of uncertain overhead cranes with high-speed hoisting motion," *IEEE Trans. Fuzzy Syst.*, vol. 22, no. 5, pp. 1262–1271, Oct. 2014.

[15] L. Ramli, Z. Mohamed, M. Ö. Efe, I. M. Lazim, and H. I. Jaafar, "Efficient swing control of an overhead crane with simultaneous payload hoisting and external disturbances," *Mech. Syst. Signal Process.*, vol. 135, Jan. 2020, Art. no. 106326.

[16] R. Liu and S. Li, "Suboptimal integral sliding mode controller design for a class of affine systems," *J. Optim. Theory Appl.*, vol. 161, no. 3, pp. 877–904, Jun. 2014.

[17] Y. Zhao and H. Gao, "Fuzzy-Model-Based control of an overhead crane with input delay and actuator saturation," *IEEE Trans. Fuzzy Syst.*, vol. 20, no. 1, pp. 181–186, Feb. 2012.

[18] W. Yu, M. A. Moreno-Armendariz, and F. O. Rodriguez, "Stable adaptive compensation with fuzzy CMAC for an overhead crane," *Inf. Sci.*, vol. 181, no. 21, pp. 4895–4907, Nov. 2011.

[19] S. Ding and Z. Wang, "Event-triggered synchronization of discrete-time neural networks: A switching approach," *Neural Netw.*, vol. 125, pp. 31–40, May 2020.

[20] L.-H. Lee, P.-H. Huang, Y.-C. Shih, T.-C. Chiang, and C.-Y. Chang, "Parallel neural network combined with sliding mode control in overhead crane control system," *J. Vib. Control*, vol. 20, no. 5, pp. 749–760, Apr. 2014.

[21] H. Chen and N. Sun, "Nonlinear control of underactuated systems subject to both actuated and unactuated state constraints with experimental verification," *IEEE Trans. Ind. Electron.*, vol. 67, no. 9, pp. 7702–7714, Oct. 2020.

[22] H. Chen, Y. Fang, and N. Sun, "A swing constrained time-optimal trajectory planning strategy for double pendulum crane systems," *Nonlinear Dyn.*, vol. 89, no. 2, pp. 1513–1524, Jul. 2017.

[23] M. Zhang, X. Ma, R. Song, X. Rong, G. Tian, X. Tian, and Y. Li, "Adaptive proportional-derivative sliding mode control law with improved transient performance for underactuated overhead crane systems," *IEEE/CAA J. Automatica Sinica*, vol. 5, no. 3, pp. 683–690, May 2018.

[24] H. Ouyang, J. Wang, G. Zhang, L. Mei, and X. Deng, "Novel adaptive hierarchical sliding mode control for trajectory tracking and load sway rejection in double-pendulum overhead cranes," *IEEE Access*, vol. 7, pp. 10353–10361, 2019.

[25] D. Qian, S. Tong, and S. Lee, "Fuzzy-Logic-based control of payloads subjected to double-pendulum motion in overhead cranes," *Autom. Construct.*, vol. 65, pp. 133–143, May 2016.

[26] L. A. Tuan, "Neural observer and adaptive fractional-order backstepping fast-terminal sliding-mode control of RTG cranes," *IEEE Trans. Ind. Electron.*, vol. 68, no. 1, pp. 434–442, Jan. 2021.

[27] J. S. Yang, M. L. Huang, W. F. Chien, and M. H. Tsai, "Application of machine vision to collision avoidance control of the overhead crane," in *Proc. Int. Conf. Electr., Autom. Mech. Eng.*, Phuket Island, Thailand, 2015, pp. 16–17.

[28] Y. Hara and Y. Noda, "Operational assistance system for obstacle collision avoidance and load sway suppression in overhead traveling crane," in *Proc. IEEE Int. Conf. Syst., Man, Cybern. (SMC)*, Budapest, Hungary, Oct. 2016, pp. 2196–2201.

[29] I. Gutierrez and J. Collado, "An LQR controller in the obstacle avoidance of a two-wires hammerhead crane," *Neurocomputing*, vol. 233, pp. 14–22, Apr. 2017.

[30] T. Miyoshi, S. Kawakami, and K. Terashima, "Path planning and obstacle avoidance considering rotary motion of load for overhead cranes," *J. Mech. Syst. Transp. Logistics*, vol. 1, no. 1, pp. 134–145, 2008.

[31] A. Inomata and Y. Noda, "Fast trajectory planning by design of initial trajectory in overhead traveling crane with considering obstacle avoidance and load vibration suppression," *J. Phys. Conf.*, vol. 744, p. 12070, 2016.

[32] S. Iftikhar, O. J. Faqir, and E. C. Kemgan, "Nonlinear model predictive control of an overhead laboratory-scale gantry crane with obstacle avoidance," in *Proc. IEEE Conf. Control Technol. Appl. (CCTA)*, Hong Kong, Aug. 2019, pp. 382–387.

[33] D. Blackburn, W. Singhose, J. Kitchen, V. Patrangenaru, J. Lawrence, T. Kamoi, and A. Taura, "Command shaping for nonlinear crane dynamics," *J. Vib. Control*, vol. 16, no. 4, pp. 477–501, Apr. 2010.

[34] D. Fujioka and W. Singhose, "Input-shaped model reference control of a nonlinear time-varying double-pendulum crane," in *Proc. 10th Asian Control Conf. (ASCC)*, May 2015, pp. 1–6.

[35] The Math Works. *MATLAB*. Accessed: 2019. [Online]. Available: https://www.mathworks.com

[36] The Math Works. *Simulink Toolbox for Use With MATLAB*. Accessed: 2019. [Online]. Available: https://www.mathworks.com/products/simulink.html

WA ZHANG received the B.S. degree from Tianjin Chengjian University, Tianjin, China, in 2016. He is currently pursuing the M.S. degree in control science and engineering with the Hebei University of Technology, Tianjin.

His major research interest includes underactuated crane system control.

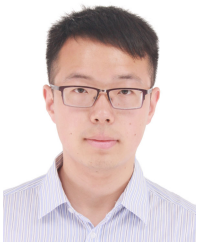

HE CHEN (Member, IEEE) received the B.S. degree in automation and the Ph.D. degree in control science and engineering from Nankai University, Tianjin, China, in 2013 and 2018, respectively.

He is currently a Lecturer of Control Science and Engineering with the School of Artificial Intelligence, Hebei University of Technology, Tianjin. His research interests include control of underactuated systems (e.g., cranes) and motion planning of wheeled mobile robots. He serves as an Academic Editor (AE) for *Mathematical Problems in Engineering*. He is also a Guest Editor for the topics *Control and Stability for Robotic Crane Systems of Frontiers Robotics and AI*.

HAIYONG CHEN received the M.S. degree from the Harbin University of Science and Technology, Harbin, China, in 2005, and the Ph.D. degree from the Institute of Automation, Chinese Academy of Sciences, Beijing, China, in 2008.

He is currently a Professor with the School of Artificial Intelligence, Hebei University of Technology, Tianjin, China. His research interests include image processing, robot vision, and pattern recognition.

WEIPENG LIU received the Ph.D. degree from the Hebei University of Technology, Tianjin, China, in 2016.

He is currently a Professor with the School of Artificial Intelligence, Hebei University of Technology, Tianjin. His research interests include image processing, artificial intelligence, robotics, and pattern recognition.